# Local Scour Mechanism around Dynamically Active Marine Structures in Non-cohesive Sediments and Unidirectional Current

M. Al-Hammadi[1]; and R. R. Simons[2]

[1]Ph.D., Dept. of Civil, Environmental and Geomatic Engineering, Univ. College London, WC1E 6BT London, U.K. (corresponding author). E-mail: mohammed.al-hammadi.13@ucl.ac.uk

[2]Professor of Fluid Mechanics and Coastal Engineering, Dept. of Civil, Environmental and Geomatic Engineering, Univ. College London, WC1E 6BT London, U.K. E-mail: r.r.simons@ucl.ac.uk

**Abstract:** This paper sheds light on the mechanism of post equilibrium seabed scour around dynamically active marine structures such as wind turbines. Exposure of a fully developed scour hole (at equilibrium state) around a wind turbine mono-pile to the cyclic movement of the structure leads to the backfilling and deformation of the scour hole. The existing approaches to scour prediction for foundation design of offshore wind turbines generally consider wind turbines as static structures and ignore the physical impact of the cyclic movement of the pile on the supporting soil and hence on the scour process. Through an experimental programme this paper explains the influence of the cyclic movement of the pile on the local scour in non-cohesive sediments. A series of flume tests at two scales were conducted. Simple hydrodynamic conditions and bed sediment configurations were adopted to highlight the effect of pile movement. The results obtained indicate that a mechanism exists by which the scour hole can be significantly deeper and wider in extent than that predicted by conventional methods. This arises through a multi-stage process consisting of periodically alternating cyclically loaded and unloaded stages simulating a sequence of storms.

**Author keywords:** Scour; Backfilling; Cyclic loading; Frequency; Current; Offshore wind turbine.

## Introduction

Strong and stable wind conditions and the development of highly efficient and reliable wind energy technology provide the motivations to expand wind farm projects into the offshore areas. However, the cost of the construction and maintenance of such projects in the marine environment is much higher than when constructed on land. Therefore, to achieve cost competitiveness it is necessary to conduct studies providing a better understanding of the unclear aspects in the current design approaches.

A key factor in the design of offshore wind turbine foundations is seabed scour. This is the erosion of mobile bed sediment from around a structure in the marine environment, and is caused by the increase in shear stress applied due to changes in the flow pattern. It can lead to problems with structural stability and makes it a challenge to design foundations for such structures.

Scour has been studied extensively since the mid-20th century, and the effects of a wide range of parameters on this process have been addressed. For instance, Whitehouse (1998), Melville and Coleman (2000), Sumer et al. (2001) and Sumer and Fredsøe (2002) present summaries of the main findings considering the scour in various sediment types, hydrodynamic conditions and foundation models. However, there is still a high level of uncertainty in the present approach to scour prediction. Jensen et al. (2006) found that even in the most conservative approaches there can still be under-prediction of scour depths.

A comparison of several scour prediction approaches is provided by Sheppard et al. (2011) using a wide range of experimental and field data. They found that some of the approaches under-predict the depth while others are conservative and noticed an improvement in the accuracy using the more recent approaches to prediction.

In another study Matutano et al. (2013) reported both over-prediction and under-prediction when predicted scour depths (using a given approach) were compared to a set of data. This is generally due to the substantial number of variables influencing the scour.

More recently, a comprehensive study on the effects of complex piers on local scour is has been carried out by Baghbadorani et al. (2018) basing their predictive approach on a set of experiments and published data. In another study Tavouktsoglou et al. (2017) investigated local scour around gravity based foundations. They adopted a novel approach based on the depth-averaged Euler number and reported good agreement with a wide range of experimental and field data.

A factor that has received little attention is the physical impact of cyclic movement of marine structures on the sea bed and its consequences for the scour process. The cylindrical structures that support wind turbines are dynamically sensitive because of their slenderness and the severe environment in which they are generally located. Wind and waves are the main sources of environmental loading and can induce cyclic movement of wind towers. Field measurements indicate that under storm conditions the nacelle (the top part of the wind tower) can experience a horizontal displacement for up to 1 m for a tower 100 m high and 5 m in diameter (Mostböck and Petryna, 2014). Wang et al. (2013) reported a similar value under extreme storm conditions including the rain load. A wide range of field data for amplitudes of cyclic movement at the bed level is provided by Long and Vanneste (1994), who quote values from less than 0.1% to more than 10% of pile diameter. Applied loading in the current test programme produced pile movements within this range of amplitude.

The majority, if not all, of the literature on scour consider the seabed around static, rigid structures. However, there have been a relatively large number of studies looking at the cyclic loading effects from structural and geotechnical points of view. Adhikari and Bhattacharya (2010), Harte et al. (2012), Bhattacharya et al. (2013), Damgaard et al. (2014), Yu et al. (2014) and Foglia et al. (2015) studied the influence of cyclic loading on sediment and the dynamic behaviour of wind turbines in the marine environment.

In one of the few studies to relate the structural behaviour to scour, Damgaard et al. (2013) investigated the effects of scour and backfilling on the natural frequency of the structure. They suggested a relationship between the variation of the structural natural frequency and the development of scour depths and backfilling heights, and found that the natural frequency can shift by about 0.02

Hz. Recently Prendergast et al. (2015) considered the change in structural natural frequency during the scour process around offshore wind turbines through scaled experiments and numerical models. Their small scale tests showed that the natural frequency could vary from less than 10 Hz to 60 Hz in the case of no scour and extreme scour depths of more than 5 times the pile diameter respectively. In their numerical model of a full scale wind turbine with a design scour depth of 1.3 times the pile diameter they observed a change in natural frequency of about 0.022 Hz. Guan et al. (2019) have carried out laboratory experiments in which they observed a reduction in depth of scour when a monopile foundation was subjected to lateral vibrations. The vibrations continued steadily throughout these tests and did not attempt to replicate the variations caused by periodic storminess.

The aim of the present study is to investigate the scour process under the influence of cyclic movement of the structure and to establish a relationship between the characteristics of structural movement and the behaviour of granular sediment.

## Methodology and Simulation

In order to investigate the influence of structural cyclic loading on the scour process a series of tests were performed. The first part of the study was conducted at relatively small scale using two circular pile diameters (D = 25 and 40 mm). Later, to confirm the results obtained from the first part, a larger pile (D = 90 mm) was tested.

### *Small scale experiments*

The first part of the study was carried out in a current flume of length of 10 m ,width of 0.3 m and depth of 0.3 m. A sediment pit (2 m long, 0.3 m wide and 0.1 m deep) was created at the centre of the flume. The distance from the upstream inlet to the sediment section was 4 m which was enough to achieve a fully developed logarithmic velocity profile at the working section. Velocity profiles were measured using a laser Doppler velocimeter (LDV) system. This device is accurate and appropriate for use in small scale flumes as it takes the measurements from outside and imposes no disturbance on the flow.

Coarse sand with a median grain size of $d_{50}$ = 0.66 mm, $\sigma = (d_{85}/ d_{15})^{0.5}$ = 1.2 and natural repose angle $\varphi$ = 29.6° (measured using direct shear tests and submerged sand piles) was employed in the test programme. The water depth in the experiments was maintained at 165 mm above the sediment section.

The pile models were manufactured in two parts. The base of the pile, of length 0.1 m, was embedded vertically in the sand and rigidly fixed to the base of the flume. It was painted with a scale rule as an indication of the scour depth through the tests. The upper part of the pile was attached to the base after preparation and levelling of the sediment section and prior to the initiation of the tests.

An electro-magnetic actuator was employed to simulate the cyclic movement of the wind turbine. This was attached rigidly to the frame of the flume and connected to the top of the pile to apply cyclic loading in the direction of flow (see Fig. 1). It was capable of applying cyclic loading up to 5 mm horizontal displacement over a wide range of frequencies.

The tests parameters were selected based on the separation of their effects on the scour process. For example, flow depth was chosen to be deep enough to minimize the influence of flow shallowness in which the vortices interact with each other. In addition, unidirectional current and clear water scour were chosen in all tests to simplify the scour so that the impact of the structural cyclic loading could be identified.

***Dynamic simulation***

Wind turbines are exposed to a variety of external excitations, as mentioned previously. The rotor, wind and waves are the main dynamic loads on such structures. These act to introduce a range of frequencies and displacements, which had to be scaled in the experiments.

The frequency of the cyclic movement is generally scaled on the natural frequency of the structure. This can be estimated by several methods; in the current study, theoretical and experimental approaches were employed. One of the formulas used widely in the estimation of the natural frequency for a fixed base pile proposed by Tempel and Molenaar (2002) can be expressed as:

$$f_1 \approx \sqrt{\frac{3.04EI}{(M+0.227\,mL)4\pi^2L^3}} \tag{1}$$

Experimentally, a set of free vibration tests were carried out on a 40 mm diameter model pile to provide an assessment of its natural frequency. The data were recorded using an accelerometer fitted at the top point of the pile. The pile was embedded in a sand bed and tested for three different free lengths. This was done by applying a small excitation to the system and recording the acceleration. This was then analysed to give its frequency. The results of the theoretical and experimental methods were in agreement, and showed that the natural frequency of the (40 mm diameter) pile with the same length and mounting employed in the flume tests was about 12 Hz.

***Soil-frequency sensitivity***

A series of preliminary tests were conducted to investigate the sensitivity of two sands with $d_{50}$ = 0.24 mm and 0.66 mm to a range of frequencies. A pile with a diameter of 40 mm was embedded vertically and fixed rigidly to the bottom of a sediment container. Five frequencies were selected from 10 to 50 Hz. All tests were carried out by application of cyclic loading for the same time (30 minutes) and the same horizontal displacement at the mudline (0.5 mm). Following the approach described by Herrick and Jones (2002) a penetrometer was used to measure the soil density at three points along the line of direction of vibration at various depths. The density was measured at 5 points on each side of the pile in the direction of loading over the entire depth. The first point was located 10 mm from the pile face to avoid the loose material in front of the pile and a distance of 50 mm was taken between each point.

The results of these tests indicate that in both sands the maximum density was achieved at 30 Hz.

***Larger scale experiments***

To confirm the results of the small scale tests a set of larger scale experiments were conducted with a 90 mm pile. These were carried out in a flume of length 20 m, 1.2 m wide and 1 m deep. A sediment pit 2.9 m long, 1.2 m wide and 0.25 m deep was constructed in the central part of the flume. Two wooden ramps of slope 1:6 were placed at the upstream and downstream ends of the sediment pit. The base of the pile was embedded at the centre of the sediment pit and fixed rigidly to the flume bottom.

Fine sand with median grain size $d_{50}$ = 0.24 mm, $\sigma = (d_{85}/ d_{15})^{0.5}$ = 1.39 and natural repose angle φ = 28.6° was employed in these tests.

All the tests were carried out in a unidirectional current and the flow depth was maintained at 450 mm. Measurements of the velocity profile through the depth were collected using a three-dimensional acoustic Doppler velocimeter (ADV). For scour monitoring, in addition to the graded pile base, which was monitored visually and by photographs during the scour development, an echo sounder device was employed. This was attached to a programmable traverse which was installed on the flume frame. By this arrangement, in addition to scour monitoring during the tests it was possible to scan the wider bed morphology after each stage of the tests.

It is worth noting that currents in the marine environment are time-varying in both direction and magnitude resulting in periods of no scour, clear water scour, and live bed scour. In live bed scour the scour hole is subjected to scouring and backfilling which can limit the development of the scour hole. Maximum depth of scour is expected to develop in the clear water regime at a flow velocity close to the sediment critical velocity, and this condition has been selected for the present study to examine the effect of structural cyclic loading on scour.

***Scour tests with low frequency cyclic loading***

In the first set of tests the frequency of cyclic loading was chosen to be 30 Hz, based on the results of the preliminary tests described above. This frequency is considerably higher than the field excitation frequencies. To investigate the scour process under a wider range of loading frequencies, further tests were carried out as described below.

These tests were conducted in the small scale current flume with a pile diameter of 25 mm. The same fine sand which was used in the larger scale tests ($d_{50}$ = 0.24 mm and φ = 28.6°) and similar water depth to the small scale tests (165 mm) were adopted in this programme. The scour was monitored visually using a graded pile base. A point gauge was also used to collect measurements of the scour hole profiles. For this set of tests, to achieve a higher amplitude of cyclic loading the pile base was hinged to the bottom of the flume.

The actuator which was employed in the small scale tests was not able to produce sufficient amplitudes across the range of frequencies required. Instead the mechanism from a shaking table was adapted to apply cyclic loading at the low frequencies required. The device was calibrated for a range of frequencies and displacements.

***Tests procedures***

The first tests looked at development of a scour hole under a unidirectional current while at the same time the pile was exposed to cyclic loading. It was noted that at the same time as scouring there was a continuous backfilling.

Based on these results it was decided to carry out a set of tests made up of multiple stages, alternating between periods with and without cyclic loading. The procedure was as follows:

1. Equilibrium stage: a normal scour hole was allowed to form around a pile without cyclic loading, under the action of a unidirectional current in an initially flat bed until an equilibrium state was achieved.
2. Cyclic loading stage: the pile was then exposed to cyclic loading. The duration of this period was scaled based on the model size. During this stage the previously developed scour hole became partially backfilled.
3. Second equilibrium stage: in this stage the cyclic loading was removed and the scour was allowed to continue until a second equilibrium depth was achieved.
4. The cyclic loading stage was repeated after the second equilibrium. This was then followed by third equilibrium and third cyclic loading stages.

As part of the overall study, tests were also carried out to investigate the effect of soil compaction on scour. In these tests the soil was compacted by application of cyclic loading for a period of 30 minutes. The compacted bed was then tested for scour in a unidirectional current.

In addition to the cases described above, low band frequencies of cyclic loading that are more reflective of the field conditions were examined. For this purpose, tests were carried out in three stages. Similar to the multi stage tests described above a typical test started by developing a scour hole in the absence of cyclic loading. After reaching equilibrium scour depth, the pile was exposed to cyclic loading. This was then followed by an un-vibrated stage during which a new scour hole was generated. For these tests the number of loading cycles was the same for each frequency; hence, depending on the frequency of cyclic loading, the time of the exposure to cyclic loading was different for each test.

### *Test conditions*

Tables 1, 2 and 3 present the test conditions adopted in this study:

Table 1 summarises the initial small scale test programme in addition to the compacted bed tests. In Tables 2 and 3 the larger scale test and the low frequency tests are presented. In Table 1 the second column presents the conditions under which the scour was developed. The term "unloaded" refers to scour development in the absence of cyclic loading, while "loaded" indicates that the pile was exposed to cyclic loading during the scouring process. Some of the tests were conducted in compacted beds as indicated "Compacted" (by application of cyclic loading giving an amplitude of 0.05 mm for 30 min.); otherwise, the bed material was at the normal density. The maximum scour depths normalised by the pile diameter are presented in the last column.

The larger scale test presented in Table 2 consisted of eight stages. The loading condition is indicated in the second column and the nondimensionalised scour depths at the upstream face of the pile are listed in the last column (similar to Table 1). All the parameters (flow depth and velocity, amplitude and frequency of cyclic loading, and duration of cyclic loading stages) were maintained at the same value throughout the multi stage test.

Table 3 summarizes the test conditions for the low frequency tests. As mentioned earlier, these tests were conducted to examine vibrations in the frequency range similar to field excitations. The same flow parameters were adopted throughout this set of tests. In addition, the number of cycles and the amplitude of the cyclic movement at the mudline were maintained at the same values for all tests.

## Results

### *Scour in compacted sands*

Fig. 2 compares the time evolution of scour in compacted sand (as a result of pile cyclic loading) (Test 4, Table 1) and in normal density sand (Test 1, Table 1). The development of each test is shown in two parts. The first hour of the test is presented on a scale of minutes, while the rest of the test is shown in hours. This is to provide more detail of the scour depths at the initial stage. The results shown in this graph indicate that the rate of scour in the compacted sand at the early stage of the test was slower than that in normal density (uncompacted) sand. However, the equilibrium states were reached in both sands at almost the same depth.

### *Scour under effect of cyclic loading*

Scour development around the cyclically loaded pile (Test 2, Table 1) is compared to that for an equivalent test in which a normal scour hole was created around a static pile (Test 1, Table 1) in Fig. 3. As for the compacted bed results, the initial hour of data was plotted separately from the rest of the data. In the loaded pile test the pile was subjected to cyclic loading once the erosion of the bed material was initiated. At the start of each test, the scour was at the same rate for both cases; however, after a few minutes, the difference in scour depths started to increase. This was due to the backfilling caused by the cyclic movement of the pile. It is worth noting that the term "backfilling" here refers to the adjustment of the steep slope upstream of the pile resulting in a slumping of sand grains to the base of the hole. In the loaded test, at the equilibrium state the scour hole was considerably shallower and wider in extent than the unloaded scour hole. As part of this process it was seen that, with cyclic loading, the slopes of the scour hole changed and formed a uniform conical shape with a slope at the natural repose angle of the sand.

### *Scour in two-stage tests*

Fig. 4 shows the results of scour depth development in a two-stage test (Test 10, Table 1) and an equivalent test without cyclic loading (Test 9, Table 1). This confirms the results above, namely that under the influence of the cyclic movement the scour hole created is shallower in depth and wider in extent. However, when the effect of cyclic loading was removed, a new deeper and smaller scour hole was developed close to the pile. The wider extent of the first stage of scour, during which the pile was subjected to cyclic loading, enabled the horseshoe vortex to reach deeper and to erode more material from the base of the previous hole. It was noted that the upstream slope of the equilibrium hole at the end of the second stage (without cyclic loading) is steeper than that developed in the unloaded test. This is attributable to the compaction of the bed sediment induced during the first (cyclic loading) stage of the test.

***Scour in multi-stage tests***

Fig. 5 shows the results of a test involving a sequence of periods of scour with and without cyclic loading (Test 14, Table 1). The test was started by development of a normal scour hole without cyclic loading until equilibrium was reached. This was followed by a stage with cyclic loading, during which the scour hole experienced backfilling and widening. After this stage the cyclic loading was stopped, and a new scour hole was generated. Once the second equilibrium was achieved the pile was exposed to a further period of cyclic loading. This procedure was repeated for seven cyclic loading stages. It was found that the exposure of the pile to periods of cyclic loading, analogous to a sequence of storms in real life, develops a deeper scour hole, in the present case more than 20% deeper than the original equilibrium scour depth. More importantly the mechanism for increasing the scour depth has the potential to continue progressively under such conditions.

In order to verify the results from this multi-stage test, a similar test was conducted at a larger scale. Fig. 6 provides the time evolution of scour at four positions around the pile. The results indicate that during the second stage, which was eight hours long, with the pile exposed to cyclic loading, the sides of the scour hole slumped into the base of the hole. After a few minutes the scour rate became higher than the backfilling (caused by the cyclic loading). Therefore, the scour depth started to increase upstream and at the sides of the pile. However, a different pattern was observed at the downstream side of the pile and the scour depth continued to decrease. This was due to the deposition of the eroded material from the front face of the pile. This material was continuously dragged under the effect of the cyclic loading to the bottom of the scour hole and later transported by the erosive vortices to the downstream side. After seven unloaded and loaded stages the scour depth recorded a significant increase in depth in comparison with the first equilibrium depth (before application of cyclic loading).

The morphology of the resulting scour holes was scanned after each stage of the test. Fig. 7 (a) and (b) compare the bed profiles after the first equilibrium (unloaded) stage (after 30 hours) and the final loaded stage (after 140 hours). The contour maps show that the scour depth as well as the area of the hole increased significantly. This was after a sequence of eight periods alternating with and without cyclic loading.

The changes caused to the scour hole during the second period (with cyclic loading) are highlighted in Fig. 8 (a). It is noticeable that the sand particles are drawn from further from the pile and have backfilled close to the structure. Similarly, Fig. 8 (b) presents the changes in scour hole during the third equilibrium stage (without cyclic loading). In this figure the generation of a new scour hole close to the pile can be observed.

***Low frequency scour tests***

Results of these tests are plotted in Fig. 9. There are 3 stages during each test: 1) scour development generated by a current over a flat bed without cyclic loading of the pile; 2) combined backfilling and scouring with cyclic loading applied; and 3) development of a new scour hole by the current without cyclic loading of the pile.

In such tests, it is important to ensure that the equilibrium state has been reached during the first stage without cyclic loading. To achieve this, after recording the maximum scour depth using the adopted equilibrium criterion, the current was allowed to run for an additional ten hours to ensure no further scour.

An equal number of loading cycles was considered in each of the four tests. Therefore, a longer test time was required for the lower frequency tests. In this programme three frequencies were tested. It was also decided to consider an additional case in which the cyclic loading stage was run with no flow taking place. This test was helpful in separating the influences of the cyclic loading and the erosion caused by the current.

In Fig. 10 the scour depth is plotted against the number of cycles applied during the cyclic loading stages starting after the equilibrium scour hole had been developed without vibration. The graph indicates two aspects of the backfilling process: 1) an initial slump of the upstream slope; 2) continuous sliding of the bed material to the base of the scour hole.

The results show that the rate of the backfilling decreases with the frequency of cyclic loading. However, with the lower frequency, a flatter scour hole was developed. This is attributable to the longer time the scour hole was exposed to the combined effects of current and cyclic loading (the longer time was necessary to apply an equal number of cycles).

Consequently, in the next period without cyclic loading, the scour depth increased as the frequency decreased (see Fig. 9). This can be explained by the flatter hole which increases the capacity of the vortices to erode more material from the base of the pile and generate a deeper hole.

In the case of the test at 1 Hz without flow (Test 3, Table 3) the backfilling recorded the greatest depth and reached an equilibrium state at the end of the cyclic loading stage (Fig. 10). The resulting scour hole was also smaller in extent relative to the equivalent test with flow (Test 2, Table 3). This was reflected in the next stage with flow and no cyclic loading, during which the equilibrium was achieved at a shallower scour depth.

**Discussion**

It is widely accepted that the slope of the upstream side of the scour hole is steeper than the natural repose angle of a non-cohesive bed sediment. Link et al. (2008) attributed this to the development of a multi-layer vortex system which provides the support and stabilises the upstream slope at a higher angle. This is in agreement with the shapes of the scour holes observed in this study (see Fig. 11. a).

Exposure of an equilibrium scour hole to horizontal movement by the pile destabilises the steep angle at the upstream side and adjusts it to the natural repose angle of the sediment through a rapid slump (see Fig. 12 a). This generates a uniform scour hole with a single slope hole in all directions around the pile.

Under the combined effects of the current and cyclic loading the scouring vortices erode the bed material from the base of the pile, while the cyclic loading continues to adjust the slope to maintain a single uniform angle slope (see Fig. 12 b and Fig. 11. b). This process is likely to continue and over time results in a wider scour hole.

In the next stage without cyclic loading the current-induced vortices develop a deeper scour hole (see Fig. 11. c). Under a sequence of loaded and unloaded stages the scour hole can reach significantly greater depths and widths, and shows no evidence of reaching an equilibrium.

The results show that the rate and magnitude of backfilling are dependent on the frequency and amplitude of the cyclic movement of the pile in addition to the current strength. This is reflected in the shape of the backfilled hole, and consequently, the generation of the second equilibrium scour hole (without cyclic loading).

This is an important finding and needs to be considered in the design of foundations for dynamically active structures (wind turbines) in the marine environment to avoid stability issues caused by the uncertainty in the prediction of scour.

## Conclusions

Results of the tests described in this paper demonstrate the significance of structural movement on the development of scour.

The main conclusions of the study are:

1. A pre-existing scour hole around a pile will tend to backfill when the pile is exposed to cyclic movement. The backfilling occurs in two stages:

a) Initial adjustment of the steep upstream slope to the natural repose angle of the sand through a rapid slump.

b) The upper layers of the adjusted slope slide continuously to stabilise and maintain a single uniform angle slope under the combined effects on erosion by the current and cyclic movement of the pile. This process is unlimited and scouring of the backfilled material is likely to continue.

2. The backfilled scour hole is wider in extent and shallower in depth in comparison with an equivalent equilibrium scour hole without cyclic loading. This increases the capacity of the erosive vortices to generate a new scour hole when the pile movement is stopped.
3. The scour hole is likely to grow significantly in both depth and extent as an unlimited process around a pile alternately static and subject to cyclic loading.
4. The same mechanism was observed over a range of frequencies of cyclic loading, at two scales and two sand sizes, for a steady current in the clear water regime.
5. It was noted that an initially compacted sand reduces the scour rate at the beginning of scour process but has no long term effect on the equilibrium scour depth.
6. The scour mechanism that was developed under effect of structural cyclic loading is likely to be observed under reversing flows induced by waves and currents.

**Acknowledgements**

This study is a part of a PhD project, funded by the Higher Committee for Education Development in Iraq (HCED-Iraq).

**Notation**

*The following symbols are used in this paper:*

$D$ = Pile diameter (m)

$d_{16}$ = Particle size at which 16% is finer (m)

$d_{50}$ = Sediment median grain size (m)

$d_{84}$ = Particle size at which 84% is finer (m)

$E$ = Young's modulus ($N/m^2$)

$f_1$ = Natural frequency of the structure (Hz)

$g$ = Gravitational acceleration ($m/sec^2$)

$h$ = Flow depth (m)

$I$ = Moment of inertia ($m^4$)

$L$ = Pile free length (m)

$m$ = Pile mass per metre (kg/m)

$M$ = Pile top mass (kg)

$S$ = Scour depth (m)

$s = \rho_s/\rho$ = ratio of sediment density to water density

$v_*$ = Friction velocity or shear velocity (m/sec)

$V$ = Depth average current velocity (m/sec)

$V_c$ = Critical current velocity (m/sec)

$\varphi$ = Natural repose angle of sand (°)

$\theta$ = Shields parameter

## References


Baghbadorani, D. A., Ataie-Ashtiani, B., Beheshti, A., Hadjzaman, M., and Jamali, M. (2018). Prediction of current-induced local scour around complex piers: Review, revisit, and integration. *Coastal Engineering*, 133, 43-58.

Bhattacharya, S., Nikitas, N., Garnsey, J., Alexander, N. A., Cox, J., Lombardi, D., and Nash, D. F. (2013). "Observed dynamic soil–structure interaction in scale testing of offshore wind turbine foundations." *Soil Dynamics and Earthquake Engineering*, 54, 47-60.

Damgaard, M., Bayat, M., Andersen, L. V., and Ibsen, L. B. (2014). "Assessment of the dynamic behaviour of saturated soil subjected to cyclic loading from offshore monopile wind turbine foundations." *Computers and Geotechnics*, 61, 116-126.

Damgaard, M., Ibsen, L. B., Andersen, L. V., and Andersen, J. K. (2013). "Cross-wind modal properties of offshore wind turbines identified by full scale testing." *Journal of Wind Engineering and Industrial Aerodynamics*, 116, 94-108.

Foglia, A., Gottardi, G., Govoni, L., and Ibsen, L. B. (2015). "Modelling the drained response of bucket foundations for offshore wind turbines under general monotonic and cyclic loading." *Applied Ocean Research*, 52, 80-91.

Guan, D., Chiew, Y-M., Melville, B. and Zheng, J. (2018). "Current-Induced Scour at Monopile Foundations Subjected to Lateral Vibrations." *Coastal Engineering*, 144, 15-21. https://doi.org/10.1016/j.coastaleng.2018.10.011

Jensen, M. S., Juul Larsen, B., Frigaard, P., DeVos, L., Christensen, E. D., Asp Hansen, E., and Bove, S. (2006). *Offshore wind turbines situated in areas with strong currents*. Offshore Center Danmark.

Herrick, J. E., and Jones, T. L. (2002). "A dynamic cone penetrometer for measuring soil penetration resistance." *Soil Science Society of America Journal*, 66(4), 1320-1324.

Link, O., Gobert, C., Manhart, M., and Zanke, U. (2008). "Effect of the horseshoe vortex system on the geometry of a developing scour hole at a cylinder." *In 4th International Conference on Scour and Erosion, Tokyo* (pp. 162-168).

Long, J.H. and Vanneste, G. (1994). Effects of cyclic lateral loads on piles in sand. Journal of Geotechnical Engineering, 120(1), pp.225-244.

Matutano, C., Negro, V., López-Gutiérrez, J., Esteban, M. D. (2013). Scour prediction and scour protections in offshore wind farms, Renewable Energy, 57, 358-365.

Melville, B. W., and Coleman, S. E. (2000). *Bridge scour*. Water Resources Publication.

Mostböck, A., and Petryna, Y. (2014). "Structural vibration monitoring of wind turbines." *In 9th International Conference on Structural Dynamics, EURODYN*.

Prendergast, L. J., Gavin, K., and Doherty, P. (2015). "An investigation into the effect of scour on the natural frequency of an offshore wind turbine." *Ocean Engineering*, 101, 1-11.

Sheppard, D. M., Melville, B. W. and Demir, H. (2011). Evaluation of existing equations for local scour at bridge piers, J. Hydraul. Eng., 140:1, 14-23.

Soulsby, R. (1997). *Dynamics of marine sands: a manual for practical applications*. Thomas Telford.

Sumer, B. M., and Fredsøe, J. (2002). *The mechanics of scour in the marine environment*. World Scientific.

Sumer, B. M., Whitehouse, R. J., and Tørum, A. (2001). "Scour around coastal structures: a summary of recent research." *Coastal Engineering*, 44(2), 153-190.

Tavouktsoglou, N.S., Harris, J.M., Simons, R.R., and Whitehouse, R.J.S. (2017) "Equilibrium Scour-Depth Prediction around Cylindrical Structures." *Journal of Waterway, Port, Coastal, and Ocean Engineering* , 143(5), Article 04017017. 10.1061/(ASCE)WW.1943-5460.0000401

van der Tempel, J., and Molenaar, D. P. (2002). "Wind turbine structural dynamics–a review of the principles for modern power generation, onshore and offshore." *Wind engineering*, 26(4), 211-222.

Wang, Z., Zhao, Y., Li, F. and Jiang, J. (2013). Extreme dynamic responses of mw-level wind turbine tower in the strong typhoon considering wind-rain loads. Mathematical Problems in Engineering, 2013.

Whitehouse, R. (1998). *Scour at marine structures: A manual for practical applications*. Thomas Telford.

Yu, L., Zhou, Q., and Liu, J. (2015). "Experimental study on the stability of plate anchors in clay under cyclic loading." *Theoretical and Applied Mechanics Letters*, 5(2), 93-96.

**List of figure captions:**

**Fig. 1.** Definition sketch of the experimental arrangement.

**Fig. 2.** Scour depth development in a compacted sand compared to the uncompacted case; d = 40 mm, $V/V_c$ = 0.96, $d_{50}$ = 0.66 mm.

**Fig. 3.** Scour depth development around static and cyclically loaded piles; D = 40 mm, $V/V_c$ = 0.96, $d_{50}$ = 0.66 mm.

**Fig. 4.** Scour depth development in a two-stage test and an equivalent normal test (without vibration); D = 25 mm, $V/V_c$ = 0.96, $d_{50}$ = 0.66 mm.

**Fig. 5.** Scour depth development in multi-stage test; D = 25 mm, $V/V_c$ = 0.94, $d_{50}$ = 0.66 mm.

**Fig. 6.** Scour depth development in the multi-stage test; D = 90 mm, $V/V_c$ = 0.93, $d_{50}$ = 0.24 mm.

**Fig. 7.** Contour maps of scour hole: a) first equilibrium (unloaded) stage (hour 31), b) fourth loaded stage (hour 144).

**Fig. 8.** Contour maps of changes in scour depth: a) during second loaded stage (hours 63 to 71), b) during third unloaded stage (hours 71 to 94).

**Fig. 9.** Scour depth development in low frequency tests; D = 25 mm, $V/V_c$ = 0.83, $d_{50}$ = 0.24 mm.

**Fig. 10.** Scour depth during backfilling and recovery caused by vibration: variation plotted against the number of load cycles applied at 3 different frequencies.

**Fig. 11.** Scour hole profiles of (Test 2 Table 3); a) after first equilibrium (unloaded) stage; b) after cyclic loading stage; c) after second equilibrium (unloaded) stage.

**Fig. 12.** Definition sketch of the changes of a scour hole profile subjected to cyclic movement of the pile through; a) changes to a fully developed equilibrium scour hole by application of the first few cycles, b) simultaneous backfilling and scouring after initial slump.

**Table 1.** Small scale test programme

| Test number | Condition | Pile diameter D (mm) | Depth averaged current velocity V (mm/s) | Flow intensity V/Vc | Shields parameter $\theta^{a}$ | Measured nondimensional scour depth S/D |
|---|---|---|---|---|---|---|
| 1 | Unloaded | 40 | 256 | 0.96 | 0.028 | 2 |
| 2 | Loaded | 40 | 256 | 0.96 | 0.028 | 1.69 |
| 3 | Loaded & Compacted | 40 | 256 | 0.96 | 0.028 | 1.7 |
| 4 | Unloaded & Compacted | 40 | 256 | 0.96 | 0.028 | 2 |
| 5 | Unloaded | 40 | 232 | 0.88 | 0.023 | 1.28 |
| 6 | Loaded<br>Unloaded | 40 | 232 | 0.88 | 0.023 | 1.09<br>1.48 |
| 7 | Loaded & Compacted<br>Unloaded & Compacted | 40 | 232 | 0.88 | 0.023 | 1.05<br>1.33 |
| 8 | Unloaded & Compacted | 40 | 232 | 0.88 | 0.023 | 1.33 |
| 9 | Unloaded | 25 | 256 | 0.96 | 0.028 | 1.6 |
| 10 | Loaded<br>Unloaded | 25 | 256 | 0.96 | 0.028 | 1.34<br>1.76 |
| 11 | Unloaded | 25 | 232 | 0.88 | 0.023 | 1.46 |
| 12 | Loaded<br>Unloaded | 25 | 232 | 0.88 | 0.023 | 1.22<br>1.68 |
| 13 | Unloaded | 25 | 250 | 0.94 | 0.027 | 1.7 |
| 14 | Multi-stage[b] | 25 | 250 | 0.94 | 0.027 | 2.14 |

Note: Flow depth h = 165 mm, Sediment median grain size $d_{50}$ = 0.66 mm, Frequency of cyclic loading = 30 Hz, Amplitude of the cyclic movement at the mudline = 0.1 mm, [a] Shields parameters calculated using Soulsby (1997) approach $\theta = v_*^2/g(s-1)d_{50}$, $v_*/V = 1/7(d_{50}/h)^{1/7}$, [b] Time of application of cyclic loading = 270 mins (see Fig.5).

**Table 2.** Larger scale test programme

| Test number | Condition | Pile diameter D (mm) | Depth averaged current velocity V (mm/s) | Flow intensity $V/V_c$ | Shields parameter $\theta$ | Sediment median grain size $d_{50}$ (mm) | Measured nondimensional scour depth S/D |
|---|---|---|---|---|---|---|---|
| 16 | Unloaded | 90 | 247 | 0.93 | 0.39 | 0.24 | 0.82 |
| | Loaded [a] | | | | | | 0.74 |
| | Unloaded | | | | | | 0.93 |
| | Loaded | | | | | | 0.78 |
| | Unloaded | | | | | | 0.94 |
| | Loaded | | | | | | 0.8 |
| | Unloaded | | | | | | 1 |
| | Loaded | | | | | | 0.82 |

Note: Flow depth h = 450 mm, Frequency of cyclic loading = 30 Hz, Amplitude of the cyclic movement at the mudline = 0.1 mm, [a] Time of application of cyclic loading = 8 hrs.

**Table 3.** Small scale low frequency test programme

| Test number | Condition | Depth averaged current velocity V (mm/s) | Flow intensity $V/V_c$ | Shields parameter θ | Frequency of cyclic loading (Hz) | Measured nondimensional scour depth S/D |
|---|---|---|---|---|---|---|
| | Unloaded | | | | | 1.92 |
| 17 | Loaded [a] | 191 | 0.83 | 0.031 | 0.3 | 1.9 |
| | Unloaded | | | | | 2.1 |
| | Unloaded | | | | | 1.92 |
| 18 | Loaded | 191 | 0.83 | 0.031 | 1 | 1.8 |
| | Unloaded | | | | | 2.06 |
| | Unloaded | | | | | 1.92 |
| 19 | Loaded (without flow) [b] | 191 | 0.83 | 0.031 | 1 | 1.6 |
| | Unloaded | | | | | 2.02 |
| | Unloaded | | | | | 1.92 |
| 20 | Loaded | 191 | 0.83 | 0.031 | 4 | 1.64 |
| | Unloaded | | | | | 2 |

Note: Flow depth h = 165 mm, Sediment median grain size $d_{50}$ = 0.24 mm, Pile diameter D = 25 mm, Amplitude of the cyclic movement at the mudline = 1 mm, [a] Applied number of cycle = 54000 cycles, [b] The current was switched off during the application of cyclic loading.

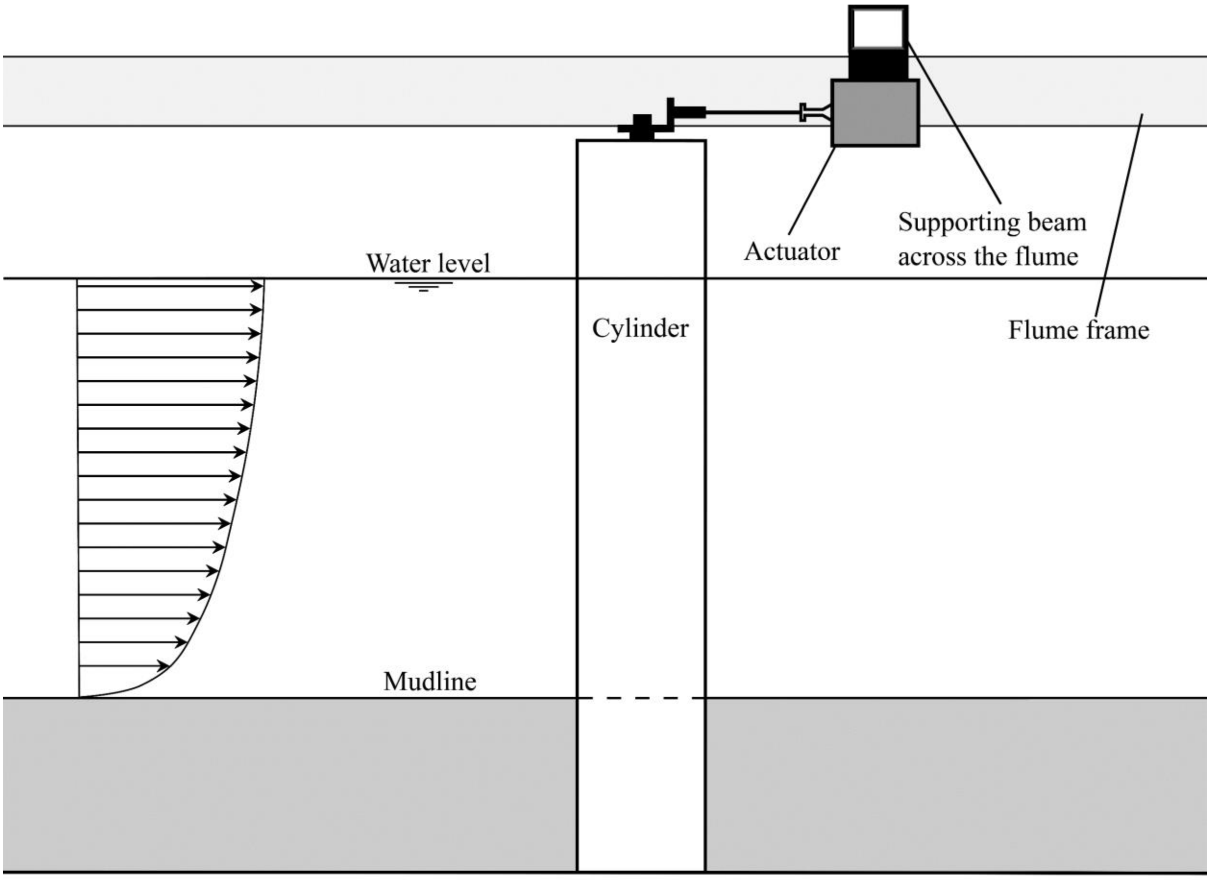


**Fig. 1.** Definition sketch of the experimental arrangement.

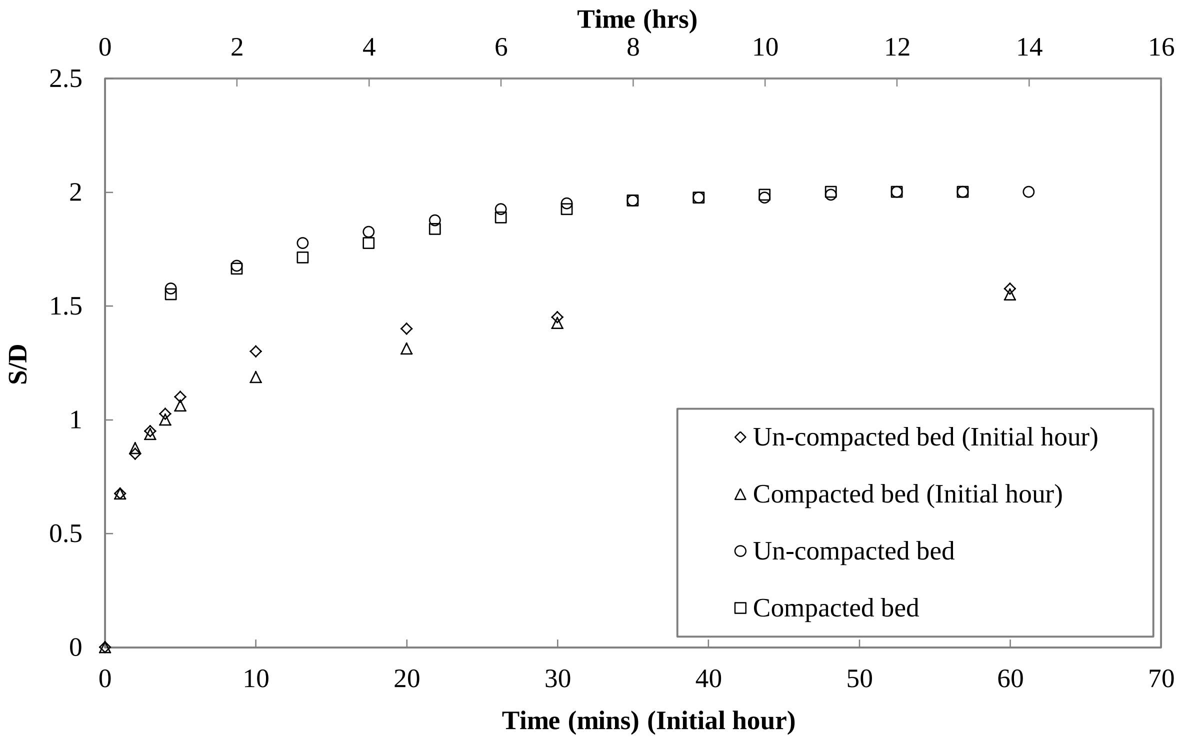


**Fig. 2.** Scour depth development in a compacted sand compared to the uncompacted case; d = 40 mm, $V/V_c = 0.96$, $d_{50} = 0.66$ mm.

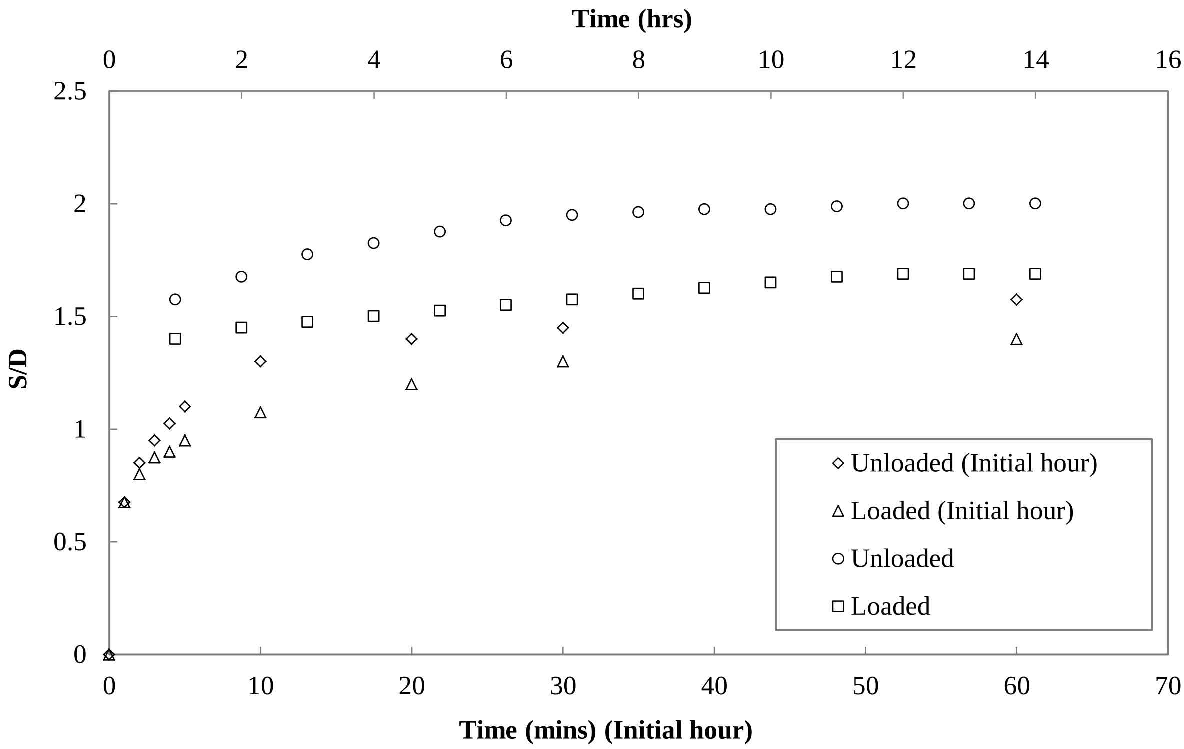


**Fig. 3.** Scour depth development around static and cyclically loaded piles; D = 40 mm, $V/V_c$ = 0.96, $d_{50}$ = 0.66 mm.

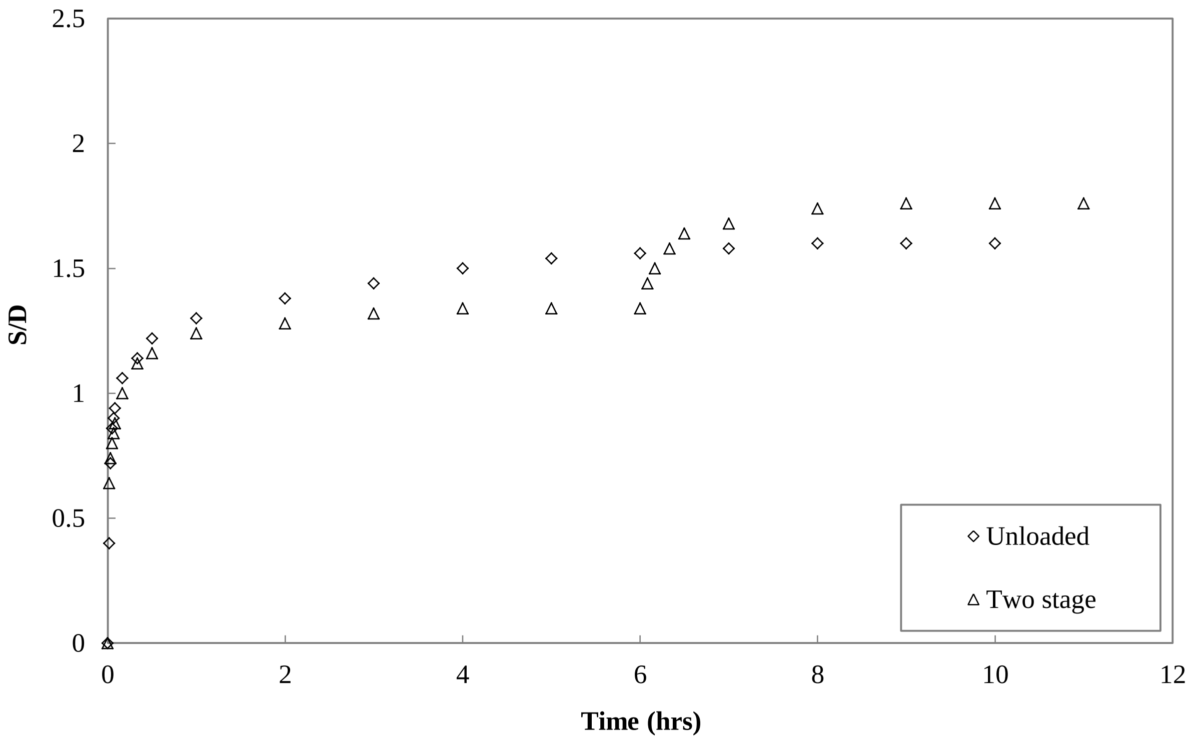


**Fig. 4.** Scour depth development in a two-stage test and an equivalent normal test (without vibration); D = 25 mm, $V/V_c$ = 0.96, $d_{50}$ = 0.66 mm.

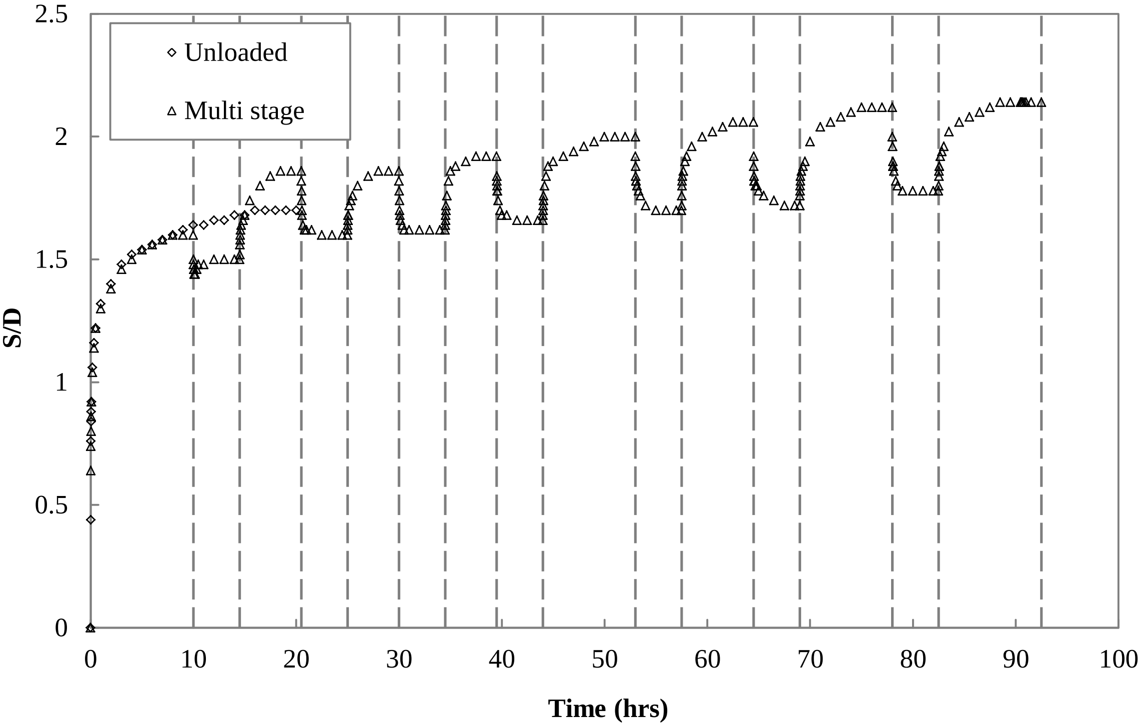


**Fig. 5.** Scour depth development in multi-stage test; D = 25 mm, $V/V_c$ = 0.94, $d_{50}$ = 0.66 mm.

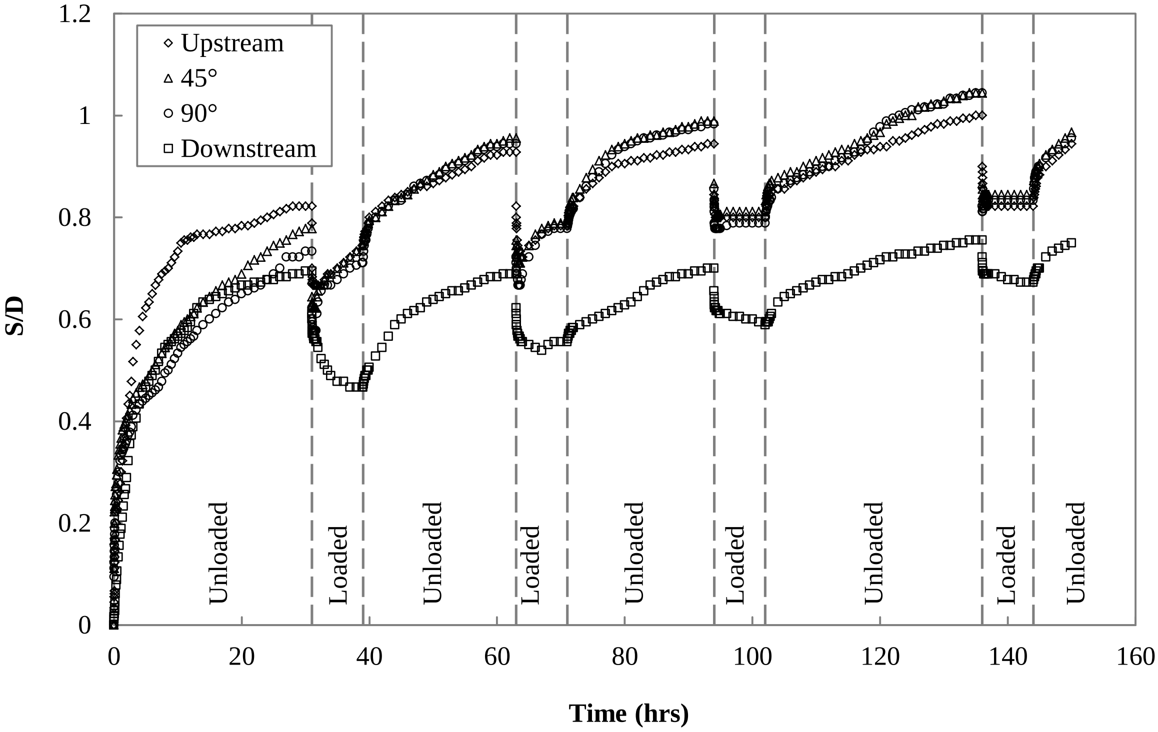


**Fig. 6.** Scour depth development in the multi-stage test; D = 90 mm, $V/V_c$ = 0.93, $d_{50}$ = 0.24 mm.

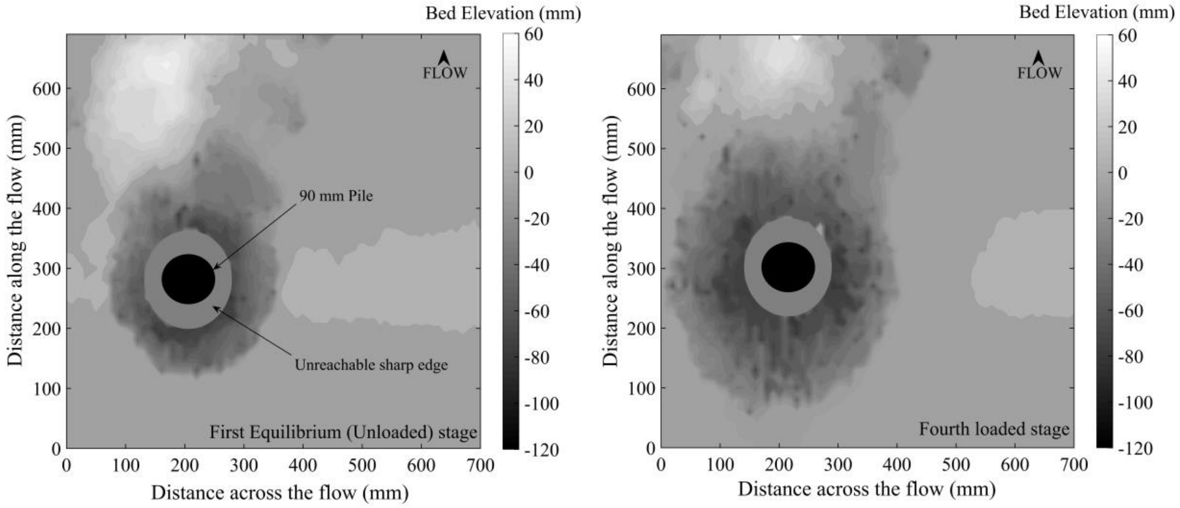


**Fig. 7.** Contour maps of scour hole: a) first equilibrium (unloaded) stage (hour 31), b) fourth loaded stage (hour 144).

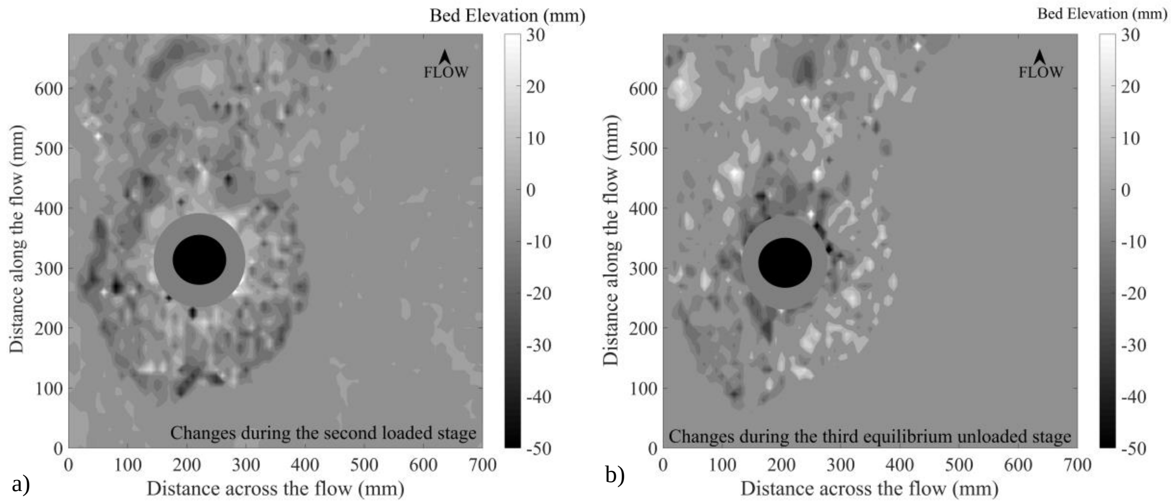


**Fig. 8.** Contour maps of changes in scour depth: a) during second loaded stage (hours 63 to 71), b) during third unloaded stage (hours 71 to 94).

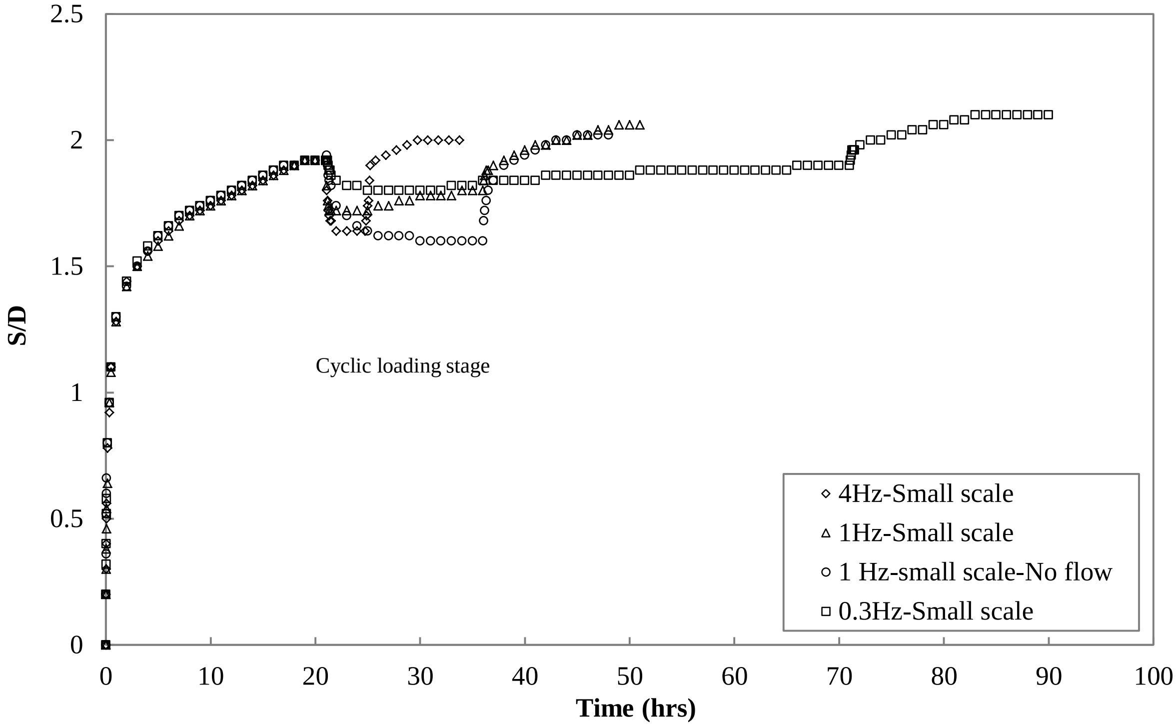


**Fig. 9.** Scour depth development in low frequency tests; D = 25 mm, $V/V_c$ = 0.83, $d_{50}$ = 0.24 mm.

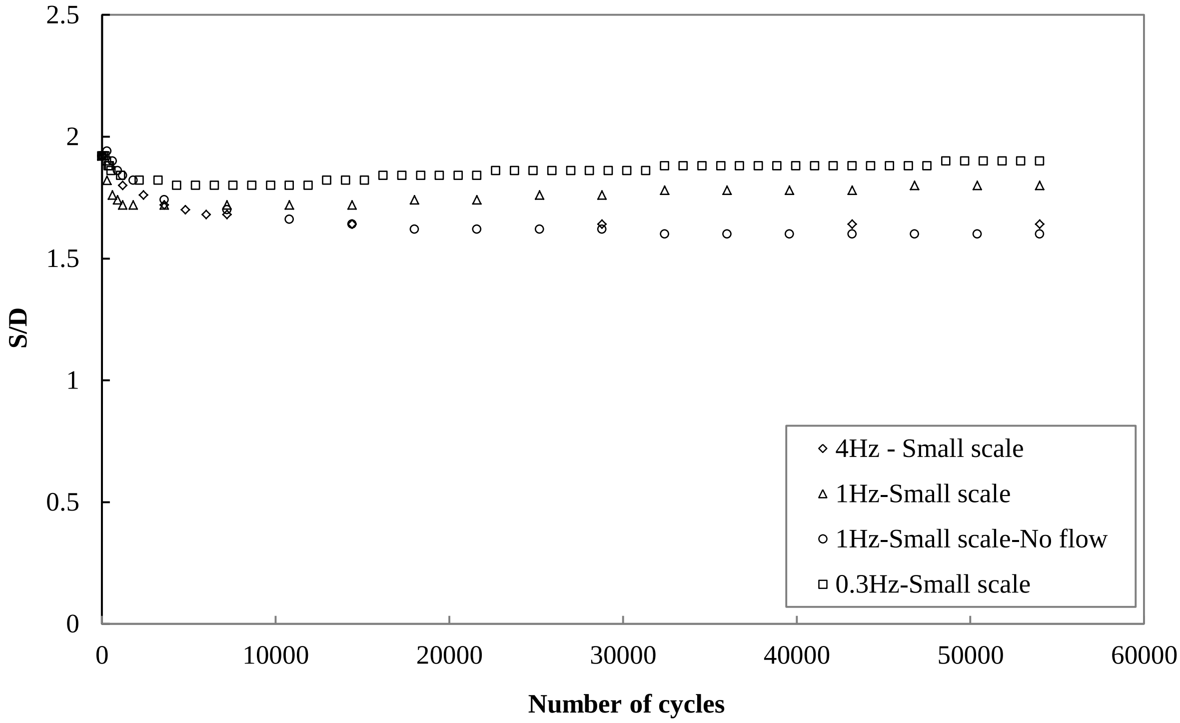


**Fig. 10.** Scour depth during backfilling and recovery caused by vibration: variation plotted against the number of load cycles applied at 3 different frequencies.

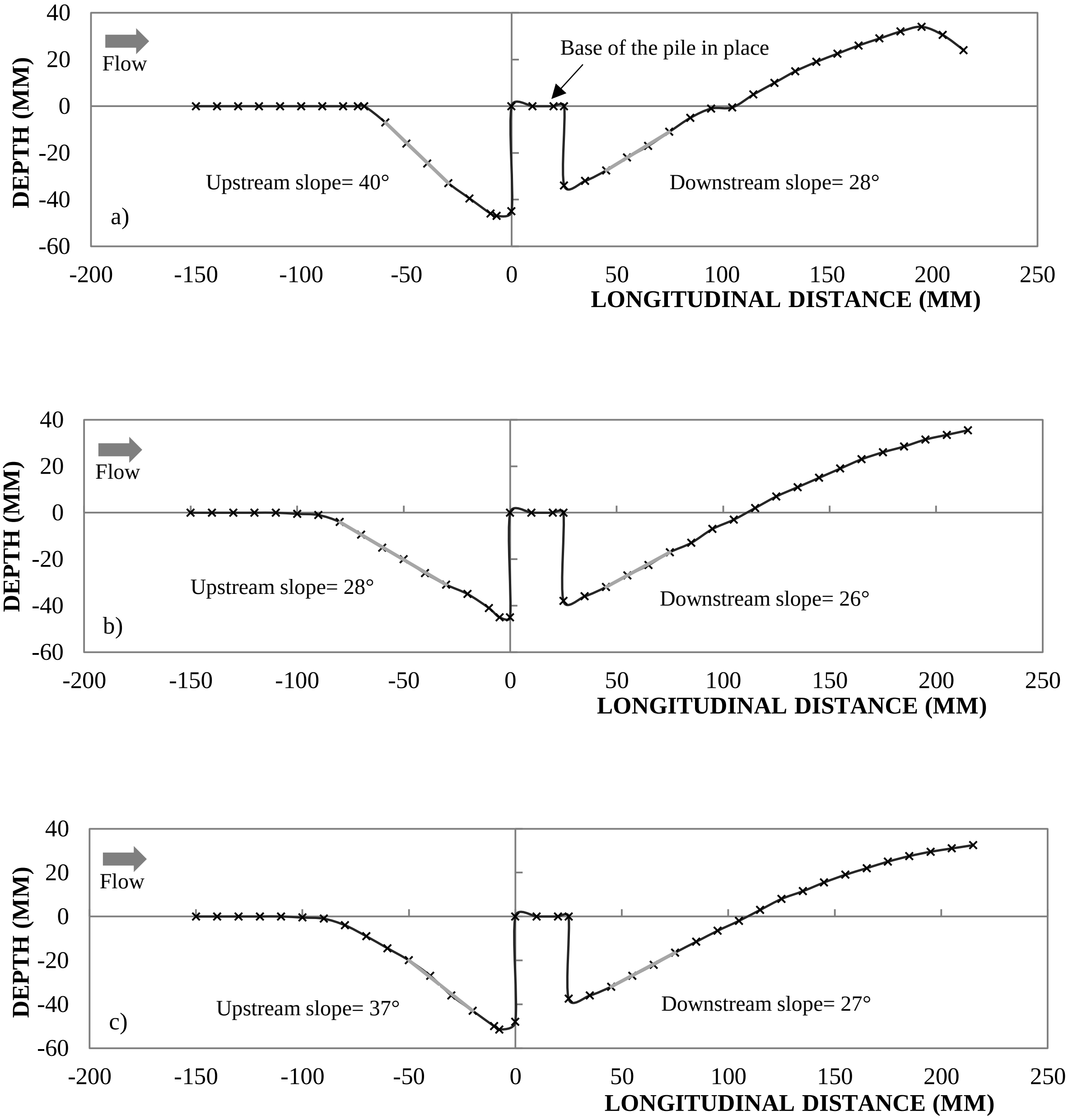


**Fig. 11.** Scour hole profiles of (Test 2 Table 3); a) after first equilibrium (unloaded) stage; b) after cyclic loading stage; c) after second equilibrium (unloaded) stage.

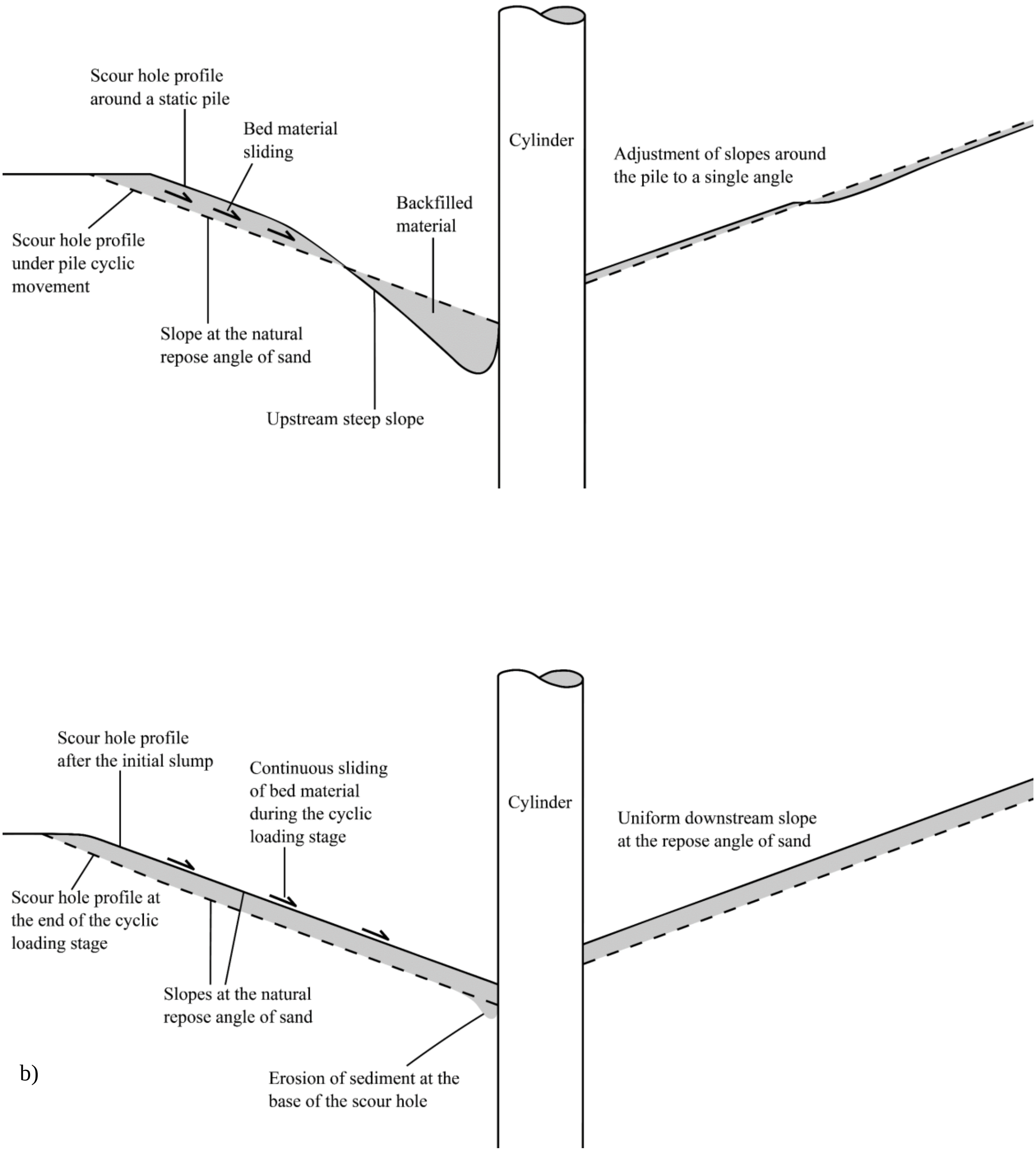


**Fig. 12.** Definition sketch of the changes of a scour hole profile subjected to cyclic movement of the pile through; a) changes to a fully developed equilibrium scour hole by application of the first few cycles, b) simultaneous backfilling and scouring after initial slump.